



How pH Modulates the Reactivity and Selectivity of a Siderophore-Associated Flavin Monooxygenase

Rosanne E. Frederick,^{†,‡} Sunil Ojha,[‡] Audrey Lamb,[§] and Jennifer L. DuBois^{*,†,‡}

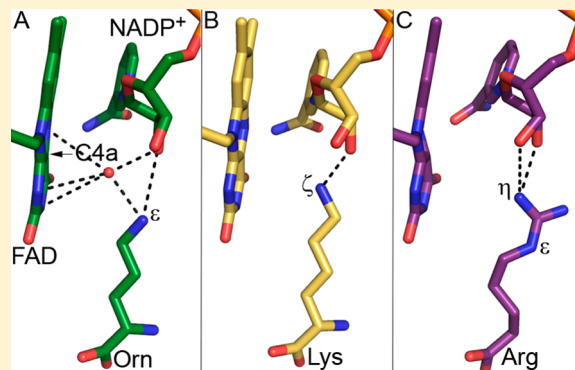
[†]Department of Chemistry and Biochemistry, University of Notre Dame, Notre Dame, Indiana 46556, United States

[‡]Department of Chemistry and Biochemistry, Montana State University, Bozeman, Montana 59715, United States

[§]Department of Molecular Biosciences, University of Kansas, Lawrence, Kansas 66045, United States

S Supporting Information

ABSTRACT: Flavin-containing monooxygenases (FMOs) catalyze the oxygenation of diverse organic molecules using O₂, NADPH, and the flavin adenine dinucleotide (FAD) cofactor. The fungal FMO SidA initiates peptidic siderophore biosynthesis via the highly selective hydroxylation of L-ornithine, while the related amino acid L-lysine is a potent effector of reaction uncoupling to generate H₂O₂. We hypothesized that protonation states could critically influence both substrate-selective hydroxylation and H₂O₂ release, and therefore undertook a study of SidA's pH-dependent reaction kinetics. Consistent with other FMOs that stabilize a C4a-OO(H) intermediate, SidA's reductive half reaction is pH independent. The rate constant for the formation of the reactive C4a-OO(H) intermediate from reduced SidA and O₂ is likewise independent of pH. However, the rate constants for C4a-OO(H) reactions, either to eliminate H₂O₂ or to hydroxylate L-Orn, were strongly pH-dependent and influenced by the nature of the bound amino acid. Solvent kinetic isotope effects of 6.6 ± 0.3 and 1.9 ± 0.2 were measured for the C4a-OOH/H₂O₂ conversion in the presence and absence of L-Lys, respectively. A model is proposed in which L-Lys accelerates H₂O₂ release via an acid–base mechanism and where side-chain position determines whether H₂O₂ or the hydroxylation product is observed.



Flavin-containing monooxygenases (FMOs) use the flavin adenine dinucleotide (FAD) cofactor and NADPH to activate and thereby unleash the oxidative power of O₂. Genome sequencing shows FMOs are widespread in all five kingdoms of life.¹ In the mammalian liver, FMOs catalyze the hydroxylation of xenobiotics that contain soft, nucleophilic groups, solubilizing them and initiating their breakdown.^{2–4} These enzymes have been shown to act on hundreds of structurally diverse substrates in an extremely nonspecific way. Bacterial, fungal, and plant FMOs share strong sequence and mechanistic similarities with the liver enzymes, though they are involved in biosynthetic pathways.¹ How the latter direct O₂ toward only the appropriate substrates, despite their similarity to the very promiscuous liver proteins, is not clear.

The bacterial *p*-hydroxy-benzoic acid hydroxylase (PHBH) is an FAD-dependent monooxygenase from a completely different sequence family which nonetheless provides an elegant paradigm for reaction control.^{5–8} Its O₂ reactivity is regulated by conformational changes that are triggered by shifts in protonation states. The substrate binds in its monoanionic form with a hydroxyl group adjacent to the site of hydroxylation. A conformational change is stimulated by deprotonation of this buried hydroxyl group, bringing FAD proximal to NADPH. Hence, FAD reduction can occur only after binding of the properly proofread substrate. The triggering proton is funneled

out of the protein via a H-bond network connecting the phenolate to a histidine at the surface of the enzyme.^{5–8} The same network of H-bonds was also shown to be important for controlling formation of the reactive C4a-OOH species which carries out an electrophilic attack on the substrate.⁸

Other well-studied FMOs involved in biodegradations, including Baeyer–Villiger monooxygenases (BVMOs),^{9,10} liver microsomal FMOs (mFMOs),¹¹ and phylogenetically distant two component monooxygenases,¹² lack a PHBH-like substrate proofreading mechanism. They rather form a kinetically stable C4a-OO(H) species that persists until a substrate arrives and reacts with it. Generating such a highly reactive intermediate without a substrate bound and in spite of the H₂O₂ that will be produced if none is available is a “bold” catalytic strategy.¹³ Hydrogen bonding interactions between the flavin isoalloxazine-N⁵H and either the amide portion of NADP or an amino acid side-chain appear to be critical for stabilizing the C4a-OO(H) against elimination of H₂O₂ or hydrolysis.¹⁴ These enzymes can be extraordinarily nonspecific for their substrates. The liver FMOs, for example, hydroxylate hundreds of structurally diverse nucleophiles.³

Received: September 10, 2013

Revised: February 3, 2014

Published: February 3, 2014



FMOs associated with siderophore biosynthesis present an unusual conundrum. They readily form a stable C4a-OO(H) in the absence of substrate, like the promiscuous liver FMOs.¹³ However, characterized siderophore-associated FMOs have exquisite specificity, largely hydroxylating only one substrate with efficiency.^{15–21} SidA is a fungal FMO that catalyzes the NADPH-dependent hydroxylation of the amine side-chain of the amino acid L-ornithine. Acetylation of the same side-chain yields a hydroxamic acid, which the fungus uses to chelate Fe(III). Three such modified amino acids are joined by nonribosomal peptide synthetases into a siderophore, which *Aspergillus fumigatus* and related fungi use for Fe uptake, intracellular trafficking, and storage. Because SidA is so important to iron metabolism in these species, it has been proposed from a biological perspective to be a potential antifungal target.^{22–24}

SidA's specificity for L-Orn in spite of its bold catalytic platform allows it to discriminate even against L-Lys, an amino acid with a side-chain that differs only by one methylene unit. L-Lys is not a substrate but, rather, dramatically destabilizes the C4a-OOH intermediate, accelerating its conversion to H₂O₂ and FAD by 150-fold.²⁵ Positively charged L-Arg, in turn, accelerates the rate of C4a-OOH formation by a similar amount while having no effect on any other catalytic step.²⁵ The recent publication of the structures of both SidA and its bacterial homologue PvdA suggests that these proteins have well-defined substrate binding pockets.^{26–29} We hypothesized and our results here confirm that the protonation states of L-Orn and L-Lys are critical regulators of reactivity in the SidA from *A. fumigatus*. A model is proposed in which L-Lys accelerates H₂O₂ release via an acid–base mechanism and where the side-chain position largely determines whether hydroxylation can occur.

■ EXPERIMENTAL PROCEDURES

Standard Procedures, Chemicals, and Equipment. All reagents were obtained from commercial sources and used without further purification unless otherwise stated. SidA from *A. fumigatus* was expressed and prepared as previously described.²⁰ Protein concentrations were routinely determined by the Bradford assay, and bound FAD (typically ~70% of the SidA monomers) was determined by UV/vis.²⁰ The buffers used were 200 mM potassium phosphate (pH 6–7.6), 200 mM Tris-SO₄ (pH 7.8–8.8), 200 mM sodium carbonate (pH 9–10). Deuterated water (D₂O, 99.9%, Cambridge Isotopes) was used to prepare buffers for solvent isotope studies, and the pD was calculated by adding 0.4 units to the measured pH. Ultrapure Milli-Q water was used in the preparation of all other reagents. Spectrophotometric and steady-state kinetic measurements were made at 25 °C using a Varian Cary 50 spectrophotometer equipped with a Peltier-style thermostat. Transient kinetics were measured with a Hi-Tech Scientific DX-2 stopped flow spectrometer with diode array detection and a continuous flow water bath at 25 °C, as described in further detail below. Data were plotted using Kaleidagraph. Data fits by nonlinear regression were produced by the same software for the steady-state data and by Kinetic Studio for the stopped-flow data. SPECFIT/32 software was used for singular value decomposition analyses.

Steady State Activity Assays. Reactions were monitored continuously via the oxidation of NADPH at 25 °C ($\lambda_{\text{max}} = 340$ nm; $\epsilon = 6220 \text{ cm}^{-1} \text{ M}^{-1}$). All reactions were initiated with ~2 μM enzyme. Enzyme was kept in the storage buffer at pH 8 and

diluted into assay buffers at the desired pH immediately prior to measurement. The ionic strength of the buffered solutions was made constant at 200 mM by addition of NaCl. Rates were referenced to the concentration of flavin-containing enzyme subunit. Specific activities are reported as 1 μM NADPH consumed s⁻¹ mg⁻¹ of SidA and are the average of three replicates.

Circular Dichroism Spectroscopy (CD). SidA (2.2 μM , 0.2 mg/mL) in a solution of 50 mM buffer at desired pH (0.2 μm -filtered) was scanned, and the ellipticity was measured on a JASCO-815 A CD spectropolarimeter from 190 to 260 nm (300 μL , 1 mm path length). Scans were measured at 50 nm/min, a response time of 1 s (DIT), and data pitch of 1.

Transient Kinetics of Reductive and Oxidative Half Reactions As a Function of pH. Reduction of the enzyme by NADPH and subsequent reactions with O₂ in the presence/absence of substrate and analogues were studied by stopped-flow spectrophotometry at 25 °C in single-mixing mode. Enzyme solutions were prepared inside a gastight tonometer and made anaerobic via repeated cycles of evacuation and purging with hydrated nitrogen or argon gas. Solutions before mixing consisted of 20–40 μM FAD-containing enzyme subunit. For studies of the reductive half reaction, the solution in the second syringe contained NADPH where the buffer was deoxygenated with Ar or N₂ via bubbling. For studies of the oxidative half reaction, a second syringe contained air-equilibrated buffer alone or aerated buffer with 15 mM of L-Orn, L-Lys, or their side-chain methylated forms. The rate constants for the formation of the C4a-OO(H) intermediate and for its reaction with either L-Orn or L-Lys are independent of whether the amino acids are supplied with the enzyme in the first syringe or with the oxygenated buffer in the second syringe, indicating that enzyme/amino acid equilibration is rapid relative to the reaction of enzyme with O₂.^{20,25}

A pH jump procedure was used to achieve desired pH values. Briefly, concentrated enzyme solutions were prepared in 20 mM Tris-SO₄ pH 8.0 and 200 mM NaCl in one syringe and mixed with a second syringe containing 200 mM buffer at close to the desired pH (6.2, 6.8, 7.2, 7.8, 8.2, 8.8, 9.2, 9.8). The final pH of each solution after mixing was determined by measurement with a pH electrode (Corning). For all studies of the oxidative half reaction in D₂O, the enzyme was first solvent exchanged into 20 mM Tris-Cl and 200 mM NaCl prepared with D₂O (pD = 8.0). The enzyme was mixed with aerated buffers prepared in D₂O with/without added L-Orn or L-Lys and having pD values the same as the pH values above. To maintain continuity between kinetic measurements, protiated Tris buffer salts were used. These are expected to add a very small amount of protons to the overall solvent and to slightly lower the measured solvent kinetic isotope effects (SKIEs) from their actual values. Hence, the SKIEs reported here are lower limits.

Reactions of SidA with NADPH as a Function of pH. Anaerobic enzyme solutions were monitored via stopped flow methods following rapid mixing with anaerobic buffer that contained 240 μM NADPH for a final NADPH concentration 120 μM in 200 mM buffer of the appropriate pH. Reactions were monitored by the disappearance of the λ_{max} 450 nm and fitted using the sum of two exponentials as described previously.^{20,25}

Data Analysis. The pH dependencies of rate constants k_{FAD} were fitted using a single-pK_a model (eq 1) (Kaleidagraph). Y represents the pH-independent value of k_{FAD} .

$$k_{\text{FAD}} = \frac{y}{1 + \frac{[\text{H}^+]}{K_a}} \quad (1)$$

Hydroxylamine Detection. Hydroxylamine products were quantified by first oxidizing them (using $\text{KI}/\text{H}_2\text{SO}_4$) to their corresponding deaminated forms plus nitrite. Control experiments using L-Orn and L-Lys indicate that their amine side-chains are not converted to nitrite. The nitrite was then analyzed using a modified form of the Griess assay,³⁰ in which the nitrite is reacted with sulfanilic acid to generate the corresponding diazonium salt. This species is then coupled with α -naphthylamine to generate a strongly absorbing azo dye. A total of 90 μL of the reaction to be analyzed was mixed with 10 μL of 0.3 M sulfuric acid. A total of 100 μL 1% (w/v) sulfanilic acid in 30% (v/v) acetic acid was added followed by 40 μL of 1.3% (w/v) potassium iodide solution in glacial acetic acid. Samples were incubated 5–7 min at room temperature. I_2 forming in the solution was cleared with 40 μL of 0.1 M sodium thiosulfate solution followed by the addition of 40 μL of 0.6% (w/v) α -naphthylamine in 30% (v/v) acetic acid and 15 min incubation. Sample absorbances were measured at 529 nm. The concentration of hydroxylated product was determined by comparison to a standard curve (0–160 μM NH_2OH).

RESULTS

Protein and Activity: Stability with pH. A plot of specific activity versus pH for SidA peaks at 8.8 and drops sharply thereafter (Figure S1, Supporting Information). The secondary structure and bound flavin content of SidA are unchanged over pH 6–10 according to the protein's CD and UV/vis spectra, respectively (data not shown). These results suggest that the protein remains intact and that changes in specific activity with pH occurring within this range are due to factors other than loss of protein structure.

Kinetics of SidA Reduction with NADPH as a Function of pH. The reaction of oxidized SidA with NADPH was monitored over pH 6–9. Kinetic traces at 450 nm were fit to the sum of two exponentials. The first phase (k_{red}) accounts for the majority of the amplitude change (Figure S2, Supporting Information). The second phase occurs with a $k = 0.2 \text{ s}^{-1}$ that is independent of NADPH concentration, the presence of substrate, or the presence of L-Arg. This phase was observed previously and may be due to a conformational change in the protein following reduction.²⁰ Neither rate constant changes appreciably over pH 6.2–9.8, either for the enzyme alone or in the presence of L-Orn, L-Lys, or L-Arg (data not shown). Similar pH-independence was observed for the reductive half reaction of cyclohexanone monooxygenase (CHMO), a Baeyer–Villiger monooxygenase (BVMO).³¹

pH Dependence of C4a-(Hydro)peroxyflavin Intermediate Formation. SidA was reduced anaerobically by titrimetric addition of 1 equiv of NADPH and then rapidly mixed with air-saturated buffers of varying pH ($K_{\text{M}}[\text{O}_2]$ for SidA = 16 μM at pH 8, 25 °C).²⁰ The formation of C4a-(hydro)peroxy intermediates (C4a-OO(H)) was monitored over time. At pH < 8.2, an intermediate with $\lambda_{\text{max}} = 369 \text{ nm}$ forms. The intermediate blue-shifts to 357 nm at pH > 8.8. It was not possible to determine an exact pK_a due to large overlap in the UV/vis spectra of the two species, though it appears to be in the 8.2–8.8 range. Similar observed shifts in the λ_{max} for this intermediate have been ascribed to the formation of C4a-OOH at lower pH and C4a-OO[−] at higher in both CHMO and

PvdA.^{19,21,31,32} The data are also consistent with a pH-dependent change in the flavin environment, due for example to movement of active site side-chains. The C4a-OO(H) intermediate forms more rapidly in the presence of L-Arg, but its decay rate is unchanged.²⁵ Hence, it is more long-lived and easier to monitor in the presence of L-Arg (Figure S3, Supporting Information).

Representative whole spectra and kinetic traces for C4a-OO(H) formation (370 nm) are shown in Figures 1 and S4,

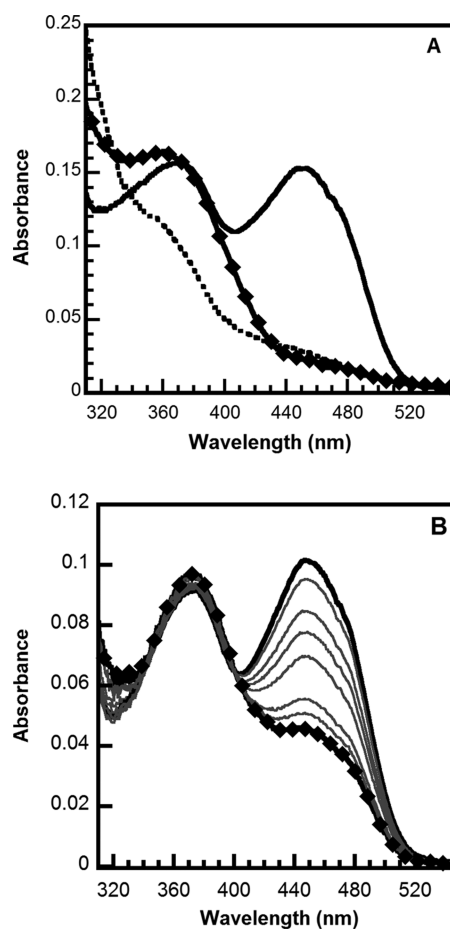


Figure 1. Spectra of species formed following rapid mixing of reduced SidA (15 μM) with O_2 -saturated buffer, illustrating intermediate formation and conversion to FAD (pH 6.2, 25 °C). (A) Reduced/FADH[−] SidA (dotted line), C4a-OOH intermediate (heavy solid line, diamonds), and oxidized/FAD SidA (heavy solid line). The spectrum of the C4a-OOH intermediate was measured 7.51 s after mixing, and the stable FAD end product after 738 s. (B) Conversion of the C4a-OOH intermediate (heavy solid line, diamonds) to oxidized FAD (heavy solid line). Spectra were measured at 7.51, 24.4, 40.9, 100, 145, 201, 351 s, and 738 s with intermediate time spectra shown in gray. Note that in this sample, some oxidation of the intermediate has already begun to occur, leading to the observed asymmetry of the spectrum relative to panel A, with added absorbance at 450 nm.

Supporting Information, respectively. Traces at 370 nm were fit with single exponential curves to derive values for $k_{\text{C4a-OOH}}$. pH has little effect on (<2-fold changes) on $k_{\text{C4a-OOH}}$ (data not shown; see R. E. Frederick, Ph.D. Thesis, University of Notre Dame.) Second-order rate constants for C4a-OOH formation were likewise pH-independent in the C2 oxidase component of *p*-hydroxyphenylacetate (HPA) 3-hydroxylase (HPAH)¹⁴ and in *p*-hydroxy-benzoic acid hydroxylase (PHBH).³³ The lack of

any acidic pH dependence suggests that the $\text{FADH}_2 \rightleftharpoons \text{FADH}^- + \text{H}^+$ equilibrium in each of these enzymes occurs with a pK_a less than 6.2, as the neutral flavin is not expected to react with O_2 .

Conversion of the Intermediate to FAD and Peroxide.

In the absence of a hydroxylation substrate, the C4a-OO(H) intermediate converts via a slow monophasic process to FAD and H_2O_2 . This conversion is characterized by an increase in the absorbance at 450 nm due to the oxidized cofactor, FAD (representative kinetic traces at 450 nm in Figure S4, Supporting Information; spectra in Figure 1). Values for first-order rate constants (k_{FAD}) exhibit a strong pH dependence (Figure 2), ranging from 0.004 s^{-1} at pH 6.2 to 0.370 s^{-1} at pH

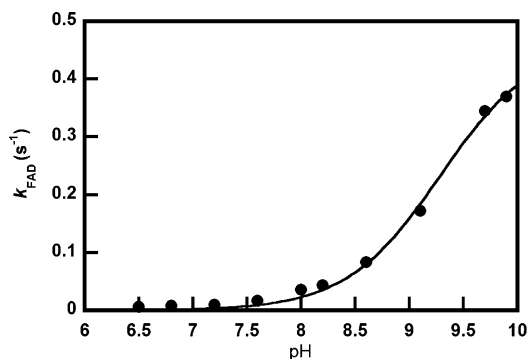


Figure 2. The rate constant for the conversion of C4a-OOH to FAD (k_{FAD}) is strongly dependent on pH. Rates constants were measured by fitting exponential curves to kinetic traces at 450 nm. A pK_a of 9.3 ± 0.1 was obtained from a fit of the data to eq 1. The average of three measurements as shown. Errors (\pm one standard deviation) here and in Figure 4 are contained within the size of the plotted data point.

9.8 (~ 2 orders of magnitude change), with a pK_a of 9.3 ± 0.05 (eq 1). It was not possible to measure the pH dependence above pH 9.5; we therefore report the pK_a as ≥ 9.3 (Table 1).

Table 1. pK_a Values for the Rate Constants for Conversion of C4a-OO(H) to FAD and Product

amino acid	pK_a
none	≥ 9.3
L-ornithine ^a	7.0 ± 0.1
<i>N</i> ⁵ -methyl-L-ornithine	8.9 ± 0.1
<i>N</i> ⁵ -dimethyl-L-ornithine	≥ 9.3
lysine ^b	7.6 ± 0.1
<i>N</i> ⁶ -methyl-L-lysine	8.2 ± 0.1
<i>N</i> ⁶ -trimethyl-L-lysine	≥ 9.3
L-arginine ^c	
L-citrulline ^c	

^aThe conversion of the intermediate to FAD in the presence of L-Orn results in hydroxylation with minimal H_2O_2 formed (see text for hydroxylation efficiencies). ^bThe conversion of the intermediate to FAD in the presence of both lysine and its analogues results in stoichiometric H_2O_2 formation. ^cArginine and citrulline have no effect on the rate or pH dependence of intermediate conversion to FAD.

Intermediate Formation in the Presence of L-Orn, L-Lys, and Their Methylated Derivatives. The reaction of NADPH-reduced SidA with O_2 was again monitored as a function of pH but in the presence of 15 mM L-Orn (substrate), L-Lys (reaction uncoupler), or their side-chain-methylated forms (Figures 3 and 4). If the proton on the C4a-

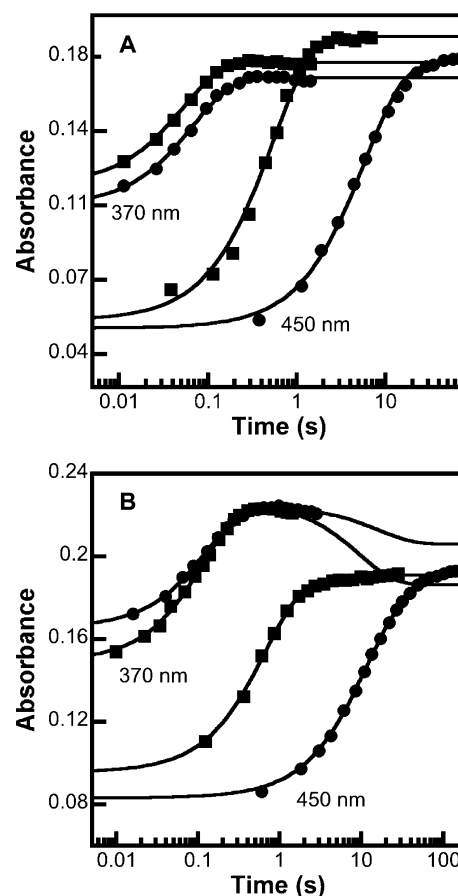


Figure 3. Representative kinetic traces for the reaction of reduced SidA with air-saturated buffer at pH 6.2 (circles) and 9.8 (squares) illustrate the effects of pH on the rates of intermediate formation (monitored at 370 nm) and conversion to FAD (450 nm) in the presence of 15 mM L-Orn (A) and 15 mM L-Lys (B). Intermediate formation does not depend on pH, while conversion to FAD in each case does. Similar data were measured in the absence of added substrate/effector. (See Supporting Information.)

OO(H) originates from the amino acid ligand (Scheme 1), the apparent rate constant for this step is expected to be faster when a ligand-derived proton is available. However, $k_{\text{C4a-OOH}}$ remains pH-independent in the presence of either L-Lys or L-Orn, suggesting that either the ligand is not the origin of the proton or that the enzyme-bound amine pK_a too high to be probed over pH 6–9.3 (data not shown).

To distinguish these possibilities, the pH profile for $k_{\text{C4a-OOH}}$ was measured in the presence of methylated L-Orn and L-Lys. Methylation of the amine maintains its positive charge, reduces the number of protons, and renders the remaining protons less acidic.³⁴ We hypothesized that, if proton donation from the ligand were needed for C4a-OO(H) formation (or breakdown), these steps should be significantly slowed in the presence of the methylated amino acids relative to their unfunctionalized counterparts. Additionally, trimethylated L-Lys has no proton available to donate to a putative C4a-OO^- . The rate constants for C4a-OO(H) formation were unchanged in the presence of L-Orn or L-Lys versus their derivatives, abbreviated here as *N*⁶-Me-L-Lys, *N*⁶-(Me)₃-L-Lys, *N*⁵-Me-L-Orn, and *N*⁵-(Me)₂-L-Orn (data not shown). The pH independence observed for $k_{\text{C4a-OOH}}$ in the absence of amino

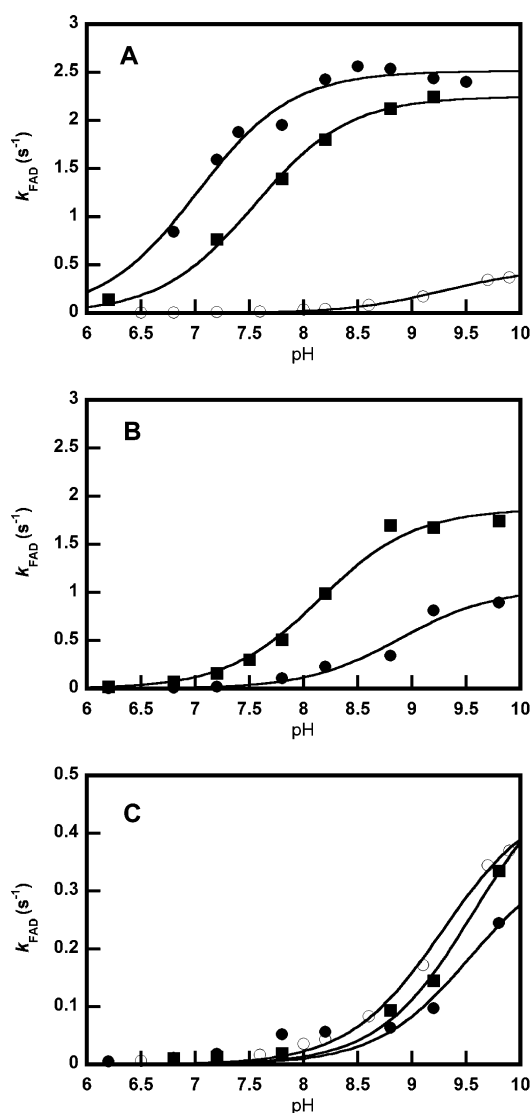


Figure 4. (A) Rate constants for the conversion of the C4a-OOH intermediate to FAD (k_{FAD}) measured in the presence of 15 mM L-Orn (closed circles) or L-Lys (closed squares). The values for k_{FAD} measured with no added amino acid (open circles) are shown on the same scale for comparison. (B) Methylation of the side-chain lowers k_{FAD} and shifts the pK_a s measured in A to more basic values, consistent with the lower nucleophilicity of the secondary amine (N^5 -Me-L-Orn: closed circles; N^6 -Me-L-Lys: closed squares). (C) The pH dependence and magnitudes of k_{FAD} for N^5 -(Me)₂-L-Orn (open circles) and N^6 -(Me)₃-L-Lys (closed squares) resemble those for the no-amino-acid case (closed circles).

acids was likewise maintained. These results suggest that the C4a-OOH proton does not come from the ligand side-chain.

C4a-OO(H) Reactions As a Function of pH. The rate constant k_{FAD} depends strongly on both pH and the nature of the added amino acid ligand (Figures 3 and 4). In 15 mM L-Lys, k_{FAD} is pH dependent with a pK_a of 7.5 ± 0.1 ; in 15 mM L-Orn, the pK_a is 7.0 ± 0.1 (Table 1, Figure 4B). These pK_a 's are each ~ 3 units below the side-chain pK_a 's for the free amino acids. Importantly, there is no basic residue in the vicinity of the substrate binding site (see Figure 5), suggesting that the observed pK_a 's are not due to a basic residue that itself acts on the bound amino acids. Both L-Orn and L-Lys destabilize the C4a-OOH to a similar extent (i.e., exhibit similar values for

k_{FAD}), though they result in two distinct reaction products (L-OrnOH versus H_2O_2).²⁵ If the observed pH dependence of k_{FAD} is due to the L-Orn or L-Lys ligand side-chain, then both facilitate C4a-OOH breakdown in their neutral forms. Neutral L-Orn-NH₂ is a better nucleophile than its positively charged counterpart and therefore is better able to attack the terminal oxygen of the C4a-OOH. Neutral L-LysNH₂ could facilitate proton transfer from the flavin-N⁵H to the C4a-OOH, catalyzing H_2O_2 production, either by physically interrupting the hydrogen bonding interaction between NADP⁺ and the flavin-N⁵H, or by acting as a base/proton shuttle between the flavin-N⁵H and C4a-OOH. The hydrogen bonding interaction between the flavin-N⁵H proton and NADP⁺ is believed to be a key mediator of C4a-OOH stability.^{10,35}

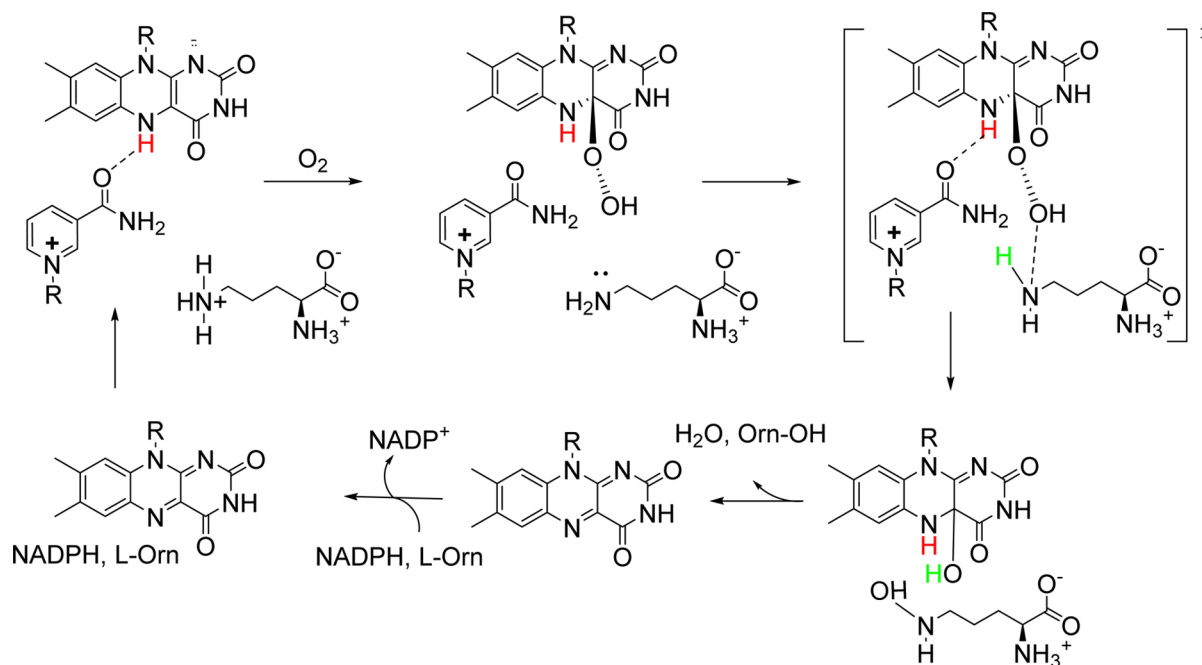
To test the hypothesis that the L-Orn/L-Lys side-chains are the origin of the observed pK_a s, pH profiles for k_{FAD} were measured in the presence of monomethylated L-Orn and L-Lys (Figure 4B). Their side-chains are expected to have a slightly elevated pK_a (~ 1 – 2 pH units) due to the electron-donating inductive effects of the methyl group on the secondary amine.³⁴ Consistent with the expected trends, the pK_a for k_{FAD} shifts from 7.0 to 8.9 ± 0.1 (ornithine) and from 7.6 to 8.2 ± 0.06 (lysine), in the presence of the methylated amino acids. The magnitudes of the measured rate constants are likewise smaller. The slower reactions could be due to steric hindrance afforded by methylating the amine or to changes in the nucleophilicity/acidity of the amine nitrogen.

To further probe the possible roles of proton transfer in L-Orn hydroxylation and in L-Lys-stimulated release of H_2O_2 , the pH dependence of k_{FAD} was measured in the presence of dimethylated L-Orn and trimethylated L-Lys (Figure 4C). Both derivatives are competitive inhibitors with L-Orn and hence can bind in the active site. However, dimethyl-L-Orn in its neutral form is expected to lack the proton which would be formally donated to the FAD–OH leaving group concomitant with the hydroxylation step (Scheme 1). Trimethyl-L-Lys is incapable of binding a proton and hence cannot act as a base. The pH profiles for k_{FAD} measured in the presence of either of these derivatives are similar to one another and to the no-substrate case: k_{FAD} has a $\text{pK}_a \geq 9.3$, a magnitude similar to that in the absence of added amino acid, and no hydroxylated product is observed.

Notably, L-citrulline and L-arginine had no effect on the pH dependence of either k_{FAD} or $k_{\text{C4a-OOH}}$ (Table 1). L-Citrulline is structurally analogous to L-Arg but has no acidic or basic side-chain groups. It is possible that the pK_a for SidA-bound L-Arg (aqueous $\text{pK}_a = 12.5$) is outside of the range attainable for SidA.

Hydroxylation Efficiency As a Function of pH. SidA's hydroxylation efficiency was measured at pH 6.2, 8.2, and 9.8 to determine whether the degree of coupling of C4a-OO(H) formation to substrate hydroxylation is affected across the pH range studied. At all three pH values, the coupling ratios ($[\text{hydroxylated product}/\text{C4a-OOH}] \times 100\%$) were nearly 100%.

Solvent Isotope Effects ($\text{H}_2\text{O}/\text{D}_2\text{O}$) on C4a-OO(H) Formation. SKIEs report on the involvement of solvent-exchangeable protons in a particular kinetic step; a SKIE is expected if proton/deuteron transfer is fully or partially rate limiting. To determine whether steps in the O_2 reaction are rate limited by proton transfers, the effect of deuterated solvent (D_2O) on $k_{\text{C4a-OOH}}$ and k_{FAD} was measured. Because enzyme solutions were allowed to equilibrate for several hours with

Scheme 1. SidA-Catalyzed Hydroxylation of L-Orn^a


^aThe flavin isoalloxazine- N^5H is shown in bold/red. The proton potentially transferred to the FAD–OH leaving group is shown in bold/green. The NADPH and flavin structures are shown in abbreviated form. The nicotinamide portion of NADPH shown in light gray could not be resolved in the crystal structure of oxidized PvdA. (See text.)

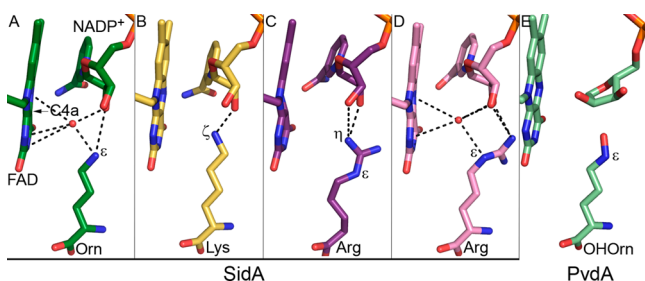


Figure 5. Ligands in the active sites of ornithine hydroxylases SidA and PvdA. (A) SidA crystallized with FAD, NADP⁺ and ornithine (PDB code: 4B63). (B) SidA crystallized with FAD, NADP⁺ and lysine (PDB code: 4B64). (C) SidA crystallized with FAD, NADP⁺ and arginine. The crystal was soaked in a solution containing dithionite (PDB code: 4B66). (D) SidA crystallized with FAD, NADP⁺, and arginine. The crystal was soaked in a solution containing dithionite and subsequently in an oxygenated solution (PDB code: 4B68). (E) Product structure of PvdA (PDB code: 3S5W). The FAD and NADP⁺ are shown as sticks and labeled only in panel A but are in consistent locations in all panels. The substrate amino acid is also shown as sticks and labeled in each panel. The water molecule hypothesized to mimic the location of the terminal oxygen in the C4a-OOH intermediate is shown as a red sphere in the relevant structures (panels A and D). The C4a carbon to which the dioxygen binds is labeled in panel A, and the ϵ , ζ , and η positions are labeled in the amino acid side-chains as required for the discussion. Figure was generated using PyMOL (W. DeLano, The PyMOL Molecular Graphics System, DeLano Scientific, San Carlos, CA, 2002).

deuterated buffers prior to measurement, all protons with exchange half-lives on the order of minutes or less (including the side-chain protons of L-Lys, L-Orn, and the flavin- N^5H) are expected to be replaced with deuterium in these measurements. In addition, the equilibration of L-Lys or L-Orn with the protein has been shown to occur rapidly relative to the reaction of

reduced enzyme with O₂.²⁰ Hence, L-Lys/L-Orn, when present, are expected to be bound to the protein.

The formation of the C4a-OOH(D) intermediate and its subsequent conversion to FAD were monitored via stopped-flow using air-saturated buffer \pm 15 mM L-Lys or L-Orn at near neutral pH/pD (6.8). The flavin and L-Lys/L-Orn are expected to be primarily in their FADH[−] and positively charged forms, respectively. The species giving rise to the optically observed pK_a between 8.2 and 8.8 (see above), attributed to either a C4a-OO[−]/C4a-OOH equilibrium or a pH-dependent active site structural rearrangement, will likewise be in its acidic form. The appearance of the spectra and the number and nature of exponential phases observed were not affected by the solvent isotope; effects were confined to the magnitudes of the measured rate constants in H₂O (k^H) versus D₂O buffer (k^D). The rate constant $k_{C4a-OOH(D)}$ in the absence of amino acid substrate/effector has a small but measurable SKIE of 1.4 ± 0.1 , lowering to 1.1 ± 0.1 in the presence of L-Lys and 1.0 ± 0.1 in the presence of L-Orn. This rate constant may encompass up to three elementary steps: the reaction between FADH[−] and O₂ to give a flavin-semiquinone/superoxide radical pair; the spin inversion and recombination of these species to form C4a-OO[−]; and the donation of a proton to this species to generate C4a-OOH. Because the third step is the only one involving a proton/deuteron, it is the most plausible candidate as the source of the small SKIE. The origin of the proton is unclear, but the kinetic data above suggest that the L-Lys/L-Orn side-chain is not its source. The small suppressive influence of L-Lys/L-Orn on the magnitude of the SKIE suggests that they interact with the proton responsible for the SKIE.

Solvent Isotope Effects (H₂O/D₂O) on C4a-OOH(D) Reactions. A small SKIE of 1.7 ± 0.05 was measured for k_{FAD} (k_{FAD}^H/k_{FAD}^D) in the presence of 15 mM L-Orn. This suggests that one of three potential microscopic steps involving proton

transfer—(1) loss of a proton from L-Orn or the flavin- N^5 , (2) transfer of a proton to the FAD-OH leaving group, or (3) hydrolysis of the FAD-OH to yield FAD—is partly rate limiting.

A similar SKIE of 1.9 ± 0.2 was measured for peroxide production from the C4a-OOH(D). Peroxide elimination could occur in a single step via direct migration of the flavin- N^5 proton to the C4a-OOH. This reaction could also involve water as a proton donor/acceptor. The SKIE increases dramatically in the presence of 15 mM L-Lys to 6.6 ± 0.3 , clearly suggesting a change in the peroxide elimination mechanism due to the presence of L-Lys with rate limiting proton transfer. The origins of the large SKIE for k_{FAD} will be further probed in a more complete study of isotope effects in future work.

DISCUSSION

FMOs involved in the biosynthesis of siderophores present two dilemmas. First, they are remarkably substrate-specific in spite of their “bold” reaction mechanism, in which a highly reactive flavin-C4a-OOH intermediate is generated even in the absence of a waiting substrate.¹³ Second, they have very different interactions with very closely related amino acids. Namely, L-Orn is SidA’s only efficient hydroxylation substrate. L-Lys, just one methylene unit longer, stimulates fast and complete uncoupling of O_2 -activation from hydroxylation, causing H_2O_2 to be emitted at a rate nearly equivalent to the rate at which L-Orn would be hydroxylated. How the protein discriminates among and executes different functions in response to these amino acids is unclear. Given their structural similarity and positive charge, we hypothesized that their protonation states and those of the enzyme could critically modulate enzyme/amino acid interactions in these FMOs. The influences of pH and solvent isotope (D_2O versus H_2O) on each of the successive steps of the reaction of SidA, a structurally characterized fungal FMO,²⁹ were therefore investigated.

The rates of FAD reduction and formation of the reactive C4a-OOH intermediate are insensitive to pH or solvent isotope over the range of pH for which the enzyme is stable. This suggests that L-Lys and L-Orn bind SidA in their positively charged forms and that intermediate formation is unaffected by the protonation states of the enzyme or substrate. L-Orn and L-Lys have a modestly stimulatory effect on the rate of O_2 activation in SidA and L-Arg a much more pronounced one, while the uncharged isostere L-citrulline has almost none.²⁵ A conserved, positively charged residue supports the initial formation of a flavin-semiquinone-superoxide radical pair in some flavin oxidases.³⁶ It is possible that the positive charge on the exogenously added amino acid side-chain, and in particular Arg with its more flexible positioning (see below), could have an analogous effect.

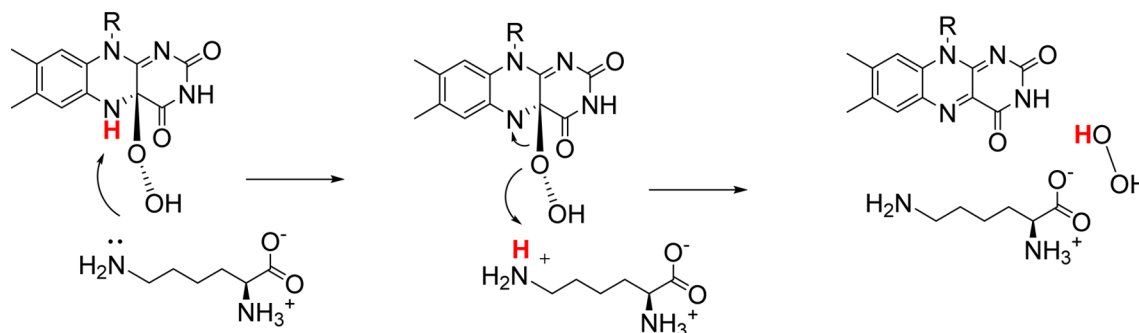
By contrast, all three of the reactions of the C4a-OOH intermediate—spontaneous elimination of H_2O_2 , production of H_2O_2 in a Lys-stimulated fashion, or hydroxylation of L-Orn—show pronounced sensitivity to pH (Figures 3 and 4). The simplest of these reactions is peroxide elimination from the C4a intermediate, which occurs very slowly when no substrate or effectors are present. This intermediate is kinetically stabilized in several flavoproteins via a hydrogen bond between the flavin- N^5H and either an active site side-chain (in C2, e.g., a serine residue) or the amide group of NADP (as seen for example in crystal structures of SidA, PAMO, PvdA, and pyranose-2-oxidase (P2O)).^{10,29,35,37,38} Hydrogen bonding prevents this key proton from migrating to the neighboring C4a-OOH,

which would lead to nonproductive generation of FAD and H_2O_2 . An analogous mechanism for H_2O_2 elimination involving the flavin- N^5H was proposed for the flavin-mono-nucleotide (FMN) dependent oxidase P2O³⁹ and supported by experiments involving transient deuterium labeling of the flavin- N^5 .⁴⁰ Similar pK_a ’s (>9.3) on the rate constant for peroxide elimination in SidA (k_{FAD}) and the C2 protein¹² and SKIEs of 2.8 (P2O) and 1.9 (SidA) further suggest that the mechanisms for H_2O_2 release may be the same in each case.

The presence of L-Lys has dramatic effects on the rate of peroxide release (described by k_{FAD}) as well as on its pH and solvent-isotope dependence, suggesting that proton transfer is integral to L-Lys’s role. The observed SKIE on k_{FAD} shifts from 1.9 to 6.6 when L-Lys is present, indicative of a distinct change in the peroxide elimination mechanism to one where a proton/deuteron transfer is rate limiting. At the same time, the pK_a for k_{FAD} shifts from >9.3 in the absence of L-Lys to 7.5 in its presence. This pK_a is roughly 3 units below the pK_a for free L-Lys and is tentatively ascribed to the L-Lys- NH_3^+ side-chain. Peroxide production is faster on the basic side of this pK_a or in the presence of neutral L-Lys- NH_2 . Hence, L-Lys does not appear to act as an acid toward the C4a-OOH. Rather, the neutral L-Lys side-chain could accelerate peroxide production by acting first as a base toward the flavin- N^5H and then as an acid toward the C4a-OOH. This mechanism is consistent with the observed pH-rate profiles for k_{FAD} in the presence of N^6 -Me-L-Lys and N^6 -(Me)₃-L-Lys. In the former case, methylation of the side-chain reduces its acidity, giving rise to the observed shift in the pK_a for k_{FAD} from 7.5 (L-Lys) to 8.1. It also results in slower H_2O_2 production (k_{FAD}), possibly due to the altered acid/base properties of the nitrogen, the need for the amine group to rotate to interact with the flavin- N^5H /C4a-OOH groups, or both. In the presence of trimethylated L-Lys, the values for k_{FAD} are no larger than in the no-amino-acid case and show a similar pH dependency. This suggests that L-Lys- $N(Me)_3^+$, a competitive inhibitor with L-Orn that can presumably bind in the active site, lacks a needed proton for it to have its effects on k_{FAD} .

When L-Orn is present, the C4a-OO(H) intermediate does not eliminate H_2O_2 but instead appears to hydroxylate an equivalent of L-Orn over the full accessible range of pH. The rate constant (k_{FAD}) for the reaction of the C4a-OO(H) intermediate to produce N^5 -hydroxy-L-Orn, H_2O , and FAD is, like peroxide elimination in the presence of L-Lys, strongly dependent on pH. In this case, the pK_a is approximately 7.0: again roughly 3 pH units below the anticipated pK_a of the free amino acid. An analogous dependence of the rate constant for the C4a-OOH/substrate reaction was observed for the PHBH from *P. aeruginosa* but not for C2, though both carry out electrophilic aromatic substitution reactions on phenolic substrates. In the former case, partial deprotonation of the phenolic -OH group is proposed to occur in the transition state for the hydroxylation reaction, making the aromatic portion of the substrate a better nucleophile toward the distal oxygen of the C4a-OOH intermediate.⁸ In the latter case, the hydroxylation itself is pH independent, but the rate constant for dehydration of the resulting flavin C4a-OH to the oxidized FMN exhibits a pK_a , above which the reaction becomes faster. The uncharged bound substrate was proposed to partially inhibit dehydration at low pH, while the corresponding anionic/deprotonated form does not.¹²

Taken together, the data suggest that L-Orn like L-Lys binds in its positively charged, side-chain protonated form. Loss of a

Scheme 2. Proposed Mechanism for L-Lys-Stimulated Elimination of H₂O₂ from C4a-OOH^a


^aThe proton derived from the flavin isoalloxazine-N⁵H and transferred via L-Lys to H₂O₂ is shown in bold/red.

proton to form the neutral L-Orn-NH₂, tentatively ascribed to the observed pK_a of 7.0 in the *k*_{FAD}/pH plot shown in Figure 4, renders the side-chain more nucleophilic toward the C4a-OOH. A second proton must be liberated from L-Orn's side-chain amine as the tetrahedral transition state breaks down (Scheme 1). Consistent with the need for the overall loss of two protons from L-Orn, the magnitude of *k*_{FAD} is greatly diminished in the presence of N⁵-(Me)₂-L-Orn, which has only one to give, and a hydroxylated product is not observed. The pH dependence of the reaction of the C4a-OOH with N⁵-(Me)₂-L-Orn is moreover similar to that observed for spontaneous C4a-OOH breakdown (Figure 4C). Each of these observations is consistent with the second ornithine-derived proton departing with the FAD-OH leaving group to generate FAD and H₂O. The moderate SKIE of 1.7 observed for the net conversion of the L-Orn and C4a-OOH to L-Orn-OH and FAD (where the FAD-OH intermediate is not observed) suggests partial rate limitation due to a step involving proton migration. For the hydroxylation reaction (Scheme 1), this step could be the loss of the Orn-NH₂ side-chain proton, formally to the FAD-O⁻ leaving group, that occurs concurrently with hydroxylation. Or, it could be the migration of the flavin-N⁵H proton to the adjacent FAD-OH, leading to loss of H₂O and production of FAD. The latter step is similar to simple C4a-OOH breakdown. The magnitude of the SKIEs for either of these steps is nearly the same.

Why the deprotonated L-Lys would act as a base toward the flavin-N⁵H, while L-Orn acts as a nucleophile toward the distal oxygen of the C4a-OOH, is not obvious. Prior work with PHBH showed that the attack angle between the substrate and the transferred oxygen atom is a critical determinant of the hydroxylation reaction.^{41–43} It is possible that, in SidA, the L-Orn side-chain is well positioned for attack of the amine lone pair on the C4a-OOH LUMO, while the slightly longer L-Lys is not. Relevant structural data exist that allow us to examine this possibility. Eight structures of SidA have been determined in different oxidation states and with different substrates/effectors (ornithine, lysine and arginine) and two have been determined for PvdA, the structural and functional homologue from *P. aeruginosa*.^{27,29} Five of these active sites are shown in Figure 5. For all of the structures, the backbone portion of the amino acid is held in place by a hydrogen bonding network that is conserved between the two proteins. Therefore, the differences among the structures are primarily in the chemical nature and placement of the amino acid side-chain, the planarity or butterfly bend of the isoalloxazine ring of the FAD for the oxidized and reduced structures, respectively, and the

orientation of the nicotinamide ring of the NADP(H). Our focus is on the placement of the side-chain; however, it should be noted that in the PvdA product structure shown here, the nicotinamide ring of the NADPH was not modeled as there was not density for this portion of the molecule, an indication that this segment of the NADPH is mobile.²⁷ It has been hypothesized that this mobility is catalytically important, allowing the nicotinamide first to assume an optimal geometry for hydride transfer to the flavin and then to form the intermediate-stabilizing hydrogen bond to the flavin N⁵H.

Comparison of the bound substrates/effectors in Figure 5 shows differences primarily at the side-chain termini that appear to reflect their different reactivities. In the SidA structure with L-Orn bound (Figure 5A), the side-chain is in an extended conformation. A water molecule is observed in proximity to the C4a of the flavin rings that has been proposed to mimic the distal oxygen of the C4a-OOH intermediate.²⁹ The ε-nitrogen of L-Orn is indeed well positioned to act as a nucleophile toward an oxygen atom in this position. The PvdA product structure with hydroxyl-L-Orn bound is shown for comparison (Figure 5E), highlighting the placement of the oxygen that was derived from the C4a-OOH and is now covalently attached to the ε-nitrogen. In the structure of SidA with lysine bound (Figure 5B), by contrast, the water molecule is not present because the ζ-nitrogen of lysine is occupying a location too close to this site (within 1.5 Å). Lysine is consequently not a substrate (does not get hydroxylated on the terminal nitrogen) because the ζ-nitrogen extends too far into the active site, where it may be better positioned to interact with the flavin-N⁵H or the flavin-proximal oxygen of the C4a-OOH, rather than the terminal -OH. This geometry of the lysine side-chain may facilitate transfer of a proton from the N⁵ of the flavin, thereby promoting the formation of H₂O₂ and giving rise to the large observed SKIE (Scheme 2).

Interestingly, the SidA structure with arginine bound (Figure 5C) also lacks the water molecule at the expected position of the electrophilic terminus of the C4a-OOH due to proximity of the η-nitrogen (less than 2 Å), and the side-chain is not fully extended. However, the ε-nitrogen can make a hydrogen bond to a water molecule in an extended geometry similar to that seen in the SidA-ornithine structure (reoxidized structure; Figure 5D). As noted above, arginine is not a substrate, but it stimulates the activation of O₂ for formation of the C4a-OOH at a rate approximately 30-fold faster relative to L-Orn or L-Lys or 150-fold faster than if no positively charged substrate or effector were present.²⁵ At the same time, unlike L-Lys, L-Arg has no effect on the rate of C4a-OOH decay to FAD and H₂O₂.

The unique properties of L-Arg may be due to a combination of several features. For example: an optimal geometry and charge for promoting activation of dioxygen to form the C4a-OOH might be achievable due to the flexibility of the arginine side-chain. The lack of a sufficiently nucleophilic nitrogen and/or the inability of the epsilon nitrogen of arginine to lose a second hydrogen (Scheme 1) prevents arginine hydroxylation, in spite of its optimal position and in spite of the fact that arginine hydroxylation is known to occur elsewhere in biochemistry, that is, in NO synthases.

CONCLUSIONS

SidA's remarkable ability to distinguish L-Orn, L-Lys, and L-Arg appears to depend on the precise positioning, the protonation states, and the nucleophilicity of each of these amino acids. While all bind in their positively charged forms, only L-Orn and L-Lys are acidic enough to deprotonate to the neutral primary amine form. The neutral amine in turn is sufficiently nucleophilic to attack the terminal oxygen of the C4a-OOH, provided that the attack angle is optimal (L-Orn, Scheme 1). Alternatively, the neutral amine, if it reaches farther toward the flavin, could act to facilitate proton transfer between the flavin-N⁵ and the C4a-OOH, catalyzing production of H₂O₂ (L-Lys, Scheme 2). While the latter proposed role for L-Lys is still speculative, the large SKIE for H₂O₂ loss specifically in the presence of L-Lys clearly indicates that a proton transfer limits this reaction's rate. The static positive charge and flexibility of the alkylguanidinium side-chain both appear to underwrite its role in promoting O₂ activation. At the same time, its poor nucleophilicity likely protects it from hydroxylation by the C4a-OOH.

SidA's ability to "feel" and respond differently to pools of structurally similar metabolites may serve some as yet unknown biological function. It is interesting to note that L-Orn, L-Lys, and L-Arg are all available in the cytosol where SidA is proposed to reside and that the composition of the free amino acid pool changes dramatically under conditions of iron stress.⁴⁴ Iron starvation also stimulates the initiation of peptidic siderophore production by SidA. It has been suggested that L-Arg can only partition away from the synthesis of essential proteins if it is present in high enough abundance.⁴⁴ Sensed sufficiency of L-Arg may be communicated to the siderophore biosynthesis pathway through SidA. By the same token, L-Lys-stimulated production of peroxide might serve some role, particularly since H₂O₂ is known to act as a signaling molecule. Plant homologues of SidA known as the yuccas initiate production of the hormone auxin, a major regulator of plant growth which is known to be generated in a spatially and temporally controlled fashion.⁴⁵ It will be of interest to see whether the yuccas likewise discriminate very similar metabolites and whether their protonation states and structures play similar roles in these important enzymes.

ASSOCIATED CONTENT

Supporting Information

Additional spectral and kinetic data referred to but not essential for the discussion of the data contained in the text. This material is available free of charge via the Internet at <http://pubs.acs.org>.

AUTHOR INFORMATION

Corresponding Author

*Phone: 540-438-6665; e-mail: jdubois@chemistry.montana.edu.

Present Address

#University of Texas at San Antonio.

Funding

Supported by National Institutes of Health Grants R01GM090260 (J.L.D.) and K02 AI093675 (ALL).

Notes

The authors declare no competing financial interest.

ACKNOWLEDGMENTS

We thank Prof Donald Kurtz (University of Texas at San Antonio) for allowing Dr. Frederick to complete her final experiments in his laboratory. We also thank Profs. Dave Ballou (University of Michigan) and Pimchai Chaiyen (Mahidol University) for helpful comments related to this manuscript. Garrett Moraski is thanked for helpful discussions.

ABBREVIATIONS

FMO, flavin monooxygenase; BVMO, Bayer–Villiger monooxygenase; FAD, flavin adenine dinucleotide; SidA, PvdA, ornithine monooxygenases; PAMO, phenylalanine monooxygenase; P2O, pyranose-2-oxidase; PHBH, para-hydroxybenzoic acid hydroxylase; FMO, flavin monooxygenase

REFERENCES

- (1) van Berkel, W. J. H., Kamerbeek, N. M., and Fraaije, M. W. (2006) Flavoprotein monooxygenases, a diverse class of oxidative biocatalysts. *J. Biotechnol.* 124, 670–689.
- (2) Poulsen, L. L., Hyslop, R. M., and Ziegler, D. M. (1979) S-Oxygenation of N-substituted thioureas catalyzed by the pig-liver microsomal FAD-containing mono-oxygenase. *Arch. Biochem. Biophys.* 198, 78–88.
- (3) Ziegler, D. M. (1988) Flavin-containing monooxygenases - catalytic mechanism and substrate specificities. *Drug Metab. Rev.* 19, 1–32.
- (4) Ziegler, D. M. (2002) An overview of the mechanism, substrate specificities, and structure of FMOs. *Drug Metab. Rev.* 34, S03–S11.
- (5) Palfey, B. A., and Massey, V. (1998) Flavin-dependent enzymes, in *Comprehensive Biological Catalysis* (Sinnott, M., Ed.) pp 83–154, Academic Press, New York.
- (6) Palfey, B. A., Moran, G. R., Entsch, B., Ballou, D. P., and Massey, V. (1999) Substrate recognition by "password" in *p*-hydroxybenzoate hydroxylase. *Biochemistry* 38, 1153–1158.
- (7) Gatti, D., Entsch, B., Ballou, D., and Ludwig, M. (1996) pH-dependent structural changes in the active site of *p*-hydroxybenzoate hydroxylase point to the importance of proton and water movements during catalysis. *Biochemistry* 35, S67–S78.
- (8) Ortiz-Maldonado, M., Entsch, B., and Ballou, D. P. (2004) Oxygen reactions in *p*-hydroxybenzoate hydroxylase utilize the H-bond network during catalysis. *Biochemistry* 43, 15246–15257.
- (9) Pazmino, D. E. T., Dudek, H. M., and Fraaije, M. W. (2010) Baeyer-Villiger monooxygenases: recent advances and future challenges. *Curr. Opin. Chem. Biol.* 14, 138–144.
- (10) Orru, R., Dudek, H. M., Martinoli, C., Pazmino, D. E. T., Royant, A., Weik, M., Fraaije, M. W., and Mattevi, A. (2011) Snapshots of enzymatic Baeyer-Villiger catalysis: Oxygen activation and intermediate stabilization. *J. Biol. Chem.* 286, 29284–29291.
- (11) Beaty, N. B., and Ballou, D. P. (1981) The oxidative half-reaction of liver microsomal FAD-containing monooxygenase. *J. Biol. Chem.* 256, 4619–4625.
- (12) Ruangchan, N., Tongsook, C., Sucharitakul, J., and Chaiyen, P. (2011) pH-dependent studies reveal an efficient hydroxylation

mechanism of the oxygenase component of *p*-hydroxyphenylacetate 3-hydroxylase. *J. Biol. Chem.* 286, 223–233.

(13) Palfey, B. A., and McDonald, C. A. (2010) Control of catalysis in flavin-dependent monooxygenases. *Arch. Biochem. Biophys.* 493, 26–36.

(14) Tongsook, C., Sucharitakul, J., Thotsaporn, K., and Chaiyen, P. (2011) Interactions with the substrate phenolic group are essential for hydroxylation by the oxygenase component of *p*-hydroxyphenylacetate 3-hydroxylase. *J. Biol. Chem.* 286, 44491–44502.

(15) Ge, L., and Seah, S. Y. K. (2006) Heterologous expression, purification, and characterization of an L-ornithine N-5-hydroxylase involved in pyoverdine siderophore biosynthesis in *Pseudomonas aeruginosa*. *J. Bacteriol.* 188, 7205–7210.

(16) Dick, S., Marrone, L., Duewel, H., Beecroft, M., McCourt, J., and Viswanatha, T. (1999) Lysine: N-6-hydroxylase: stability and interaction with ligands. *J. Protein Chem.* 18, 893–903.

(17) Thariath, A. M., Fatum, K. L., Valvano, M. A., and Viswanatha, T. (1993) Physicochemical characterization of a recombinant cytoplasmic form of lysine-N6-hydroxylase. *Biochim. Biophys. Acta* 1203, 27–35.

(18) Chocklett, S. W., and Sobrado, P. (2010) *Aspergillus fumigatus* SidA is a highly specific ornithine hydroxylase with bound flavin cofactor. *Biochemistry* 49, 6777–6783.

(19) Meneely, K. M., and Lamb, A. L. (2007) Biochemical characterization of a flavin adenine dinucleotide-dependent monooxygenase, ornithine hydroxylase from *Pseudomonas aeruginosa*, suggests a novel reaction mechanism. *Biochemistry* 46, 11930–11937.

(20) Mayfield, J. A., Frederick, R. E., Streit, B. R., Wenciewicz, T. A., Ballou, D. P., and DuBois, J. L. (2010) Comprehensive spectroscopic, steady state, and transient kinetic studies of a representative siderophore-associated flavin monooxygenase. *J. Biol. Chem.* 285, 30375–30388.

(21) Meneely, K. M., Barr, E. W., Bollinger, J. M., Jr., and Lamb, A. L. (2009) Kinetic mechanism of ornithine hydroxylase (PvdA) from *Pseudomonas aeruginosa*: Substrate triggering of O(2) addition but not flavin reduction. *Biochemistry* 48, 4371–4376.

(22) Schrettel, M., Bignell, E., Kragl, C., Sabiha, Y., Loss, O., Eisendle, M., Wallner, A., Arst, H. N., Haynes, K., and Haas, H. (2007) Distinct roles for intra- and extracellular siderophores during *Aspergillus fumigatus* infection. *PLoS Pathogens* 3, 1195–1207.

(23) Haas, H. (2012) Iron - a key nexus in the virulence of *Aspergillus fumigatus*. *Front. Microbiol.* 3, 28.

(24) Schrettel, M., Bignell, E., Kragl, C., Joechl, C., Rogers, T., Arst, H. N., Haynes, K., and Haas, H. (2004) Siderophore biosynthesis but not reductive iron assimilation is essential for *Aspergillus fumigatus* virulence. *J. Exp. Med.* 200, 1213–1219.

(25) Frederick, R. E., Mayfield, J. A., and DuBois, J. L. (2011) Regulated O(2) activation in flavin-dependent monooxygenases. *J. Am. Chem. Soc.* 133, 12338–12341.

(26) Olucha, J., Meneely, K. M., Chilton, A. S., and Lamb, A. L. (2011) Two structures of an N-hydroxylating flavoprotein monooxygenase: ornithine hydroxylase from *Pseudomonas aeruginosa*. *J. Biol. Chem.* 286, 31789–31798.

(27) Olucha, J., and Lamb, A. L. (2011) Mechanistic and structural studies of the N-hydroxylating flavoprotein monooxygenases. *Bioorg. Chem.* 39, 171–177.

(28) Olucha, J., Meneely, K. M., Chilton, A. S., and Lamb, A. L. (2011) Two structures of an N-hydroxylating flavoprotein monooxygenase: ornithine hydroxylase from *Pseudomonas aeruginosa*. *J. Biol. Chem.* 286, 31789–31798.

(29) Franceschini, S., Fedkenheuer, M., Vogelaar, N. J., Robinson, H. H., Sobrado, P., and Mattevi, A. (2012) Structural insight into the mechanism of oxygen activation and substrate selectivity of flavin-dependent N-hydroxylating monooxygenases. *Biochemistry* 51, 7043–7045.

(30) Tomlinson, G., Cruickshank, W. H., and Viswanatha, T. (1971) Sensitivity of substituted hydroxylamines to determination by iodine oxidation. *Anal. Biochem.* 44, 670–679.

(31) Sheng, D. W., Ballou, D. P., and Massey, V. (2001) Mechanistic studies of cyclohexanone monooxygenase: Chemical properties of intermediates involved in catalysis. *Biochemistry* 40, 11156–11167.

(32) DuBois, J. L., and Klinman, J. P. (2006) Role of a strictly conserved active site tyrosine in cofactor genesis in the copper amine oxidase from *Hansenula polymorpha*. *Biochemistry* 45, 3178–3188.

(33) Ortiz-Maldonado, M., Gatti, D., Ballou, D. P., and Massey, V. (1999) Structure-function correlations of the reaction of reduced nicotinamide analogues with *p*-hydroxybenzoate hydroxylase substituted with a series of 8-substituted flavins. *Biochemistry* 38, 16636–16647.

(34) Hall, H. K., Jr. (1957) Correlation of the base strengths of amines. *J. Am. Chem. Soc.* 79, 5441–5444.

(35) Thotsaporn, K., Chenprakhon, P., Sucharitakul, J., Mattevi, A., and Chaiyen, P. (2011) Stabilization of C4a-hydroperoxyflavin in a two-component flavin-dependent monooxygenase is achieved through interactions at flavin N5 and C4a atoms. *J. Biol. Chem.* 286, 28170–28180.

(36) Gadda, G. (2012) Oxygen activation in flavoprotein oxidases: the importance of being positive. *Biochemistry* 51, 2662–2669.

(37) Orru, R., Pazmino, D. E. T., Fraaije, M. W., and Mattevi, A. (2010) Joint functions of protein residues and NADP(H) in oxygen activation by flavin-containing monooxygenase. *J. Biol. Chem.* 285, 35021–35028.

(38) Sucharitakul, J., Prongjit, M., Haltrich, D., and Chaiyen, P. (2008) Detection of a C4a-hydroperoxyflavin intermediate in the reaction of a flavoprotein oxidase RID A-8236–2010. *Biochemistry* 47, 8485–8490.

(39) Sucharitakul, J., Wongnate, T., and Chaiyen, P. (2011) Hydrogen peroxide elimination from C4a-hydroperoxyflavin in a flavoprotein oxidase occurs through a single proton transfer from flavin N5 to a peroxide leaving group. *J. Biol. Chem.* 286, 16900–16909.

(40) Sucharitakul, J., Wongnate, T., and Chaiyen, P. (2010) Kinetic isotope effects on the noncovalent flavin mutant protein of pyranose 2-oxidase reveal insights into the flavin reduction mechanism RID A-8236–2010. *Biochemistry* 49, 3753–3765.

(41) Schreuder, H. A., Hol, W. G. J., and Drenth, J. (1990) Analysis of the active-site of the flavoprotein para-hydroxybenzoate hydroxylase and some ideas with respect to its reaction-mechanism. *Biochemistry* 29, 3101–3108.

(42) Schreuder, H. A., Hol, W. G. J., and Drenth, J. (1988) Molecular modeling reveals the possible importance of a carbonyl oxygen binding pocket for the catalytic mechanism of para-hydroxybenzoate hydroxylase. *J. Biol. Chem.* 263, 3131–3136.

(43) Ballou, D. P., Entsch, B., and Cole, L. J. (2005) Dynamics involved in catalysis by single-component and two-component flavin-dependent aromatic hydroxylases. *Biochem. Biophys. Res. Commun.* 338, 590–598.

(44) Schrettel, M., Beckmann, N., Varga, J., Heinekamp, T., Jacobsen, I. D., Jochl, C., Moussa, T. A., Wang, S., Gsaller, F., Blatzer, M., Werner, E. R., Niermann, W. C., Brakhage, A. A., and Haas, H. (2010) HapX-mediated adaption to iron starvation is crucial for virulence of *Aspergillus fumigatus*. *PLoS Pathogens* 6, e1001124.

(45) Dai, X., Mashiguchi, K., Chen, Q., Kasahara, H., Kamiya, Y., Ojha, S., DuBois, J., Ballou, D., and Zhao, Y. (2013) The biochemical mechanism of auxin biosynthesis by an *Arabidopsis* yucca flavin-containing monooxygenase. *J. Biol. Chem.* 288, 1448–1457.